Thermochimica Acta, 188 (1991) 1–15
Elsevier Science Publishers B.V., Amsterdam

DSC sample temperature control while measuring reaction kinetics [α]

Gibson L. Batch[1] and Christopher W. Macosko

Department of Chemical Engineering and Materials Science, University of Minnesota, Minneapolis, MN 55455 (USA)

(Received 25 September 1989)

Abstract

Although DSC has been used extensively in the literature to measure the degree of cure and reaction kinetics, relatively little work has been performed to assess the limitations and accuracy of the DSC principle itself. The purpose of this paper is to examine two inherent limitations of DSC; control of sample temperature and measurement of heat flow. These limitations are a result of (1) the low thermal conductivity of the polymer sample, (2) heat transfer resistance at the interface between the pan and the sample holder, and (3) time lags inherent in the DSC control mechanism. These three contributions were examined in experiment and theory for a power compensated DSC with several types of sample pans. Procedures are presented for determining (a) the time lag of the DSC control mechanism, (b) the heat flow limit for a 1°C mean temperature change for a given sample and pan geometry, (c) an estimate of the mean temperature increase for a given exothermic heat flow, and (d) a correction for time lags in both the sample and DSC instrumentation. Dynamic DSC runs are shown to involve large sample temperature increases which may distort the calorimetric data. Inaccuracies due to large heat flow can be avoided by using either lower temperature or smaller samples.

INTRODUCTION

Differential scanning calorimetry (DSC) measures heat flow from a sample while controlling the temperature to a specified program. The advantages of DSC are its simplicity, ease of use, control of sample temperature, and its ability to measure the rate of reaction, extent of reaction and heat capacity on the same sample. The reaction rate is assumed to be proportional to the rate of heat release from the sample. Unlike other analytical techniques, DSC directly measures the rate of conversion for liquid, gel, and solid states. Disadvantages in DSC are an insensitivity to slow reaction rates and an inability to distinguish simultaneous chemical reactions.

[α] Presented at the 18th NATAS Conference, San Diego, CA, September 24–27, 1989.
[1] Present address: 3M Corp., St. Paul, MN 55144, USA.

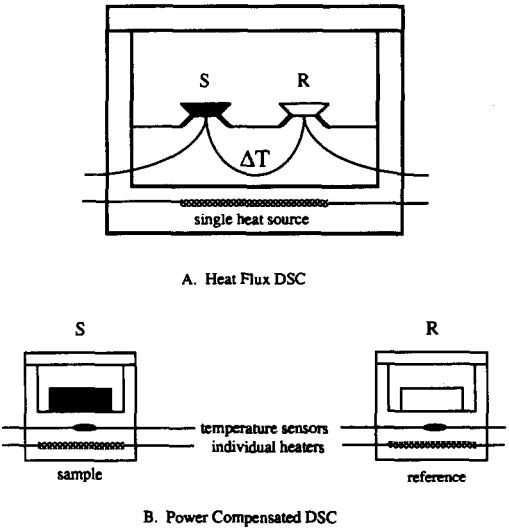

Fig. 1. Two types of differential scanning calorimeters.

DSC systems operate by either the heat flux or the power compensated principle (see Fig. 1) [1–3]. In heat flux DSC, sample and reference pans are exposed to a single heat source, and the sample heat flow is proportional to a measured temperature difference. In power compensated DSC, the sample and reference are heated in separate furnaces. Differential heat flow is measured directly by the differential energy to the furnaces, while a control system maintains both sample and reference cells at nearly the same temperature.

DSC runs are either isothermal or dynamic, the latter involving a linear increase in temperature with time, e.g.

$$T(t) = T_0 + St \tag{1}$$

where S is the temperature scanning rate in K min^{-1}. Dynamic DSC data are sometimes used to determine kinetic parameters [4–10]; however, isothermal DSC data are generally preferred because kinetic rate constants are easier to evaluate, changing the heat capacity with cure does not affect results, and changing kinetic mechanisms with temperature do not confound exotherm peaks for any single run [3]. Isothermal DSC has often been used for measuring reaction kinetics of step and chain polymerizations [5,9–18]. One disadvantage of isothermal experiments is that an initial start-up period of 1–3 min is necessary to equilibrate the DSC system at the testing temperature. If samples begin to react before thermal equilibrium is reached, part of the heat of reaction will be undetected by the DSC. Corrections for undetected heat flow may be estimated by extrapolation [19–22], or by performing DSC experiments at lower temperature.

Other systematic errors in measuring heat flow and temperature by DSC have received little attention. Duswalt [23] defined a critical sample thickness for thermal runaway based on first-order reaction kinetics. This analysis is incomplete, however, because temperature errors may be significant without thermal runaway, and in many cases first-order kinetics do not apply. Gonzalez and Shen [24] numerically modeled the DSC sample using a transient equation of heat conduction, but this approach ignores time lags in the DSC control mechanism [25] and it is difficult to implement.

This paper will examine systematic errors in DSC calorimetric measurements and sample temperature. Heat transfer resistance in a DSC sample will be predicted using an analytical heat transfer model. Melting point experiments with indium will verify the model and evaluate heat transfer characteristics of several types of sample pans. The response time of the DSC temperature control system itself will be determined by measuring the change in melting temperature with scanning rate. An example will show how this analysis may be used to evaluate the mean temperature increase during a run and the amount of time lag in the calorimetric data. Recommendations to reduce systematic heat flow and temperature errors are discussed.

THEORETICAL

The endothermic heat flow measured by DSC, h, is ideally equal to the exothermic heat flow from the sample q (e.g. $h = -q$). In reality, however, $-q$ is sometimes different to h owing to non-idealities of the DSC. For power compensated DSC, the energy balance [26] around the sample is

$$-q = h - (C_s - C_r)S + \tau_{lag}\frac{dh}{dt} \tag{2}$$

sample heat flow = measured heat flow − heat capacity mismatch + conduction lag

where the second term on the right-hand side is due to heat capacity mismatch between sample and reference and the third term is a correction for the time lag between a thermal event and detection by the DSC. The DSC time constant τ_{lag} should be small if q is to be measured accurately. The τ_{lag} term has two contributions; one from the resistance between the sample pan and the sample holder and one from delays in the DSC heat flow control loop

$$\tau_{lag} = \tau_{DSC} + R_{gap}(m_p C_p + m_s C_s) \tag{3}$$

DSC Lag + gap resistance lag

where τ_{DSC} is the lag time of the DSC controller, m_p and C_p are the mass and specific heat of the sample pan, m_s and C_s are those of the sample, and R_{gap} is the thermal resistance between the sample pan and the pan holder (Fig. 2). Since τ_{DSC}, m_p, C_p and C_s are fixed, τ_{lag} can only be reduced by

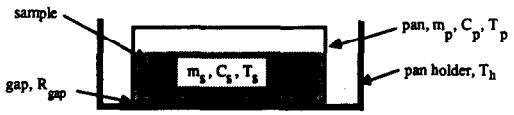

Fig. 2. Schematic of DSC sample pan and sample pan holder.

decreasing m_s or R_{gap}. The R_{gap} value would be smallest if no pans were used at all. Most samples, however, would foul the heat transfer surfaces, so small aluminum sample pans are used which are easily weighed and inserted into and removed from the DSC. Sealed pans also prevent sample loss by evaporation.

Temperature control is important for DSC samples with large reaction exotherms. The heat of cure causes an increase in temperature and hence increases the rate of polymerization (autothermal acceleration). Acceleration is enhanced by samples with low thermal conductivity, a large heat of reaction, and large reaction activation energies. The difference between the sample temperature T_s and the temperature recorded by the DSC, T_{DSC}, is

$$\Delta T_{DSC} \equiv T_{DSC} - T_s = \underset{\substack{\text{dynamic}\\\text{lag}}}{2S\tau_{lag}} - \underset{\substack{\text{gap}\\\text{resistance}}}{qR_{gap}} - \underset{\substack{\text{sample}\\\text{resistance}}}{qR_{sample}} \tag{4}$$

where the first term is the lag for dynamic runs only, and the second and third terms are intrinsic temperature differences across resistances at the gap and sample, respectively (Fig. 3). Because a time lag in a dynamic run will occur both towards and away from the sample, the dynamic lag term of eqn. (4) is doubled.

The sample heat transfer resistance causes the temperature to vary from the wall to the center of the sample. If heat conduction can be assumed to be at pseudo-steady state (i.e. transients within the sample are neglected), then the equation for heat transfer to be solved analytically (see Appendix), resulting in a closed form equation for R_{sample}, is

$$R_{sample} = \frac{4}{\pi^5} f(W) \frac{W}{ck_s r_0} \tag{5}$$

where c is the lid contact parameter ($c = 1$ when the sample does not touch the lid and $c = 4$ if it does), $f(W)$ depends on the sample aspect ratio

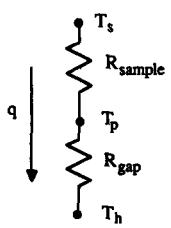

Fig. 3. Schematic of heat flow resistances from a DSC sample during an isothermal run.

($W = m_s/\rho\pi r_0^3$), r_0 is the sample radius, and k_s is the sample thermal conductivity. From eqn. (4), R_{sample} would be zero in the limit of zero sample mass. Under isothermal conditions ($S = 0$), the mean temperature increase is a function of q and m_s:

$$\Delta T_{DSC} = q\left[R_{gap} + R_{sample}(m_s)\right] \tag{6}$$

One could alternatively use eqn. (6) to determine the maximum allowable heat flow q_{max} which has ΔT_{DSC} less than some limiting value, ΔT_{limit}:

$$q_{max} = \frac{\Delta T_{limit}}{R_{sample} + R_{gap}} \tag{7}$$

In the present work the τ_{DSC} and R_{gap} values for several types of sample pan were measured. Equations (2) and (7) will then be used to determine errors in heat flow and temperature for typical DSC data.

EXPERIMENTAL

Four types of sample pan are studied in this paper (Fig. 4). Standard pans (Perkin–Elmer part number 0219–0041) are intended for solid samples, but they can be used for liquids with low vapor pressure at the testing temperature. The lid of the standard pan contacts the sample. Volatile pans (Perkin–Elmer part number 0219–0062) have a volume of 25 μl and can withstand internal pressure up to 45 p.s.i.g. Hermetic pans (Du Pont part number 900794–901) can also withstand internal pressure up to 45 p.s.i.g., and they can be sealed with the lid either upright (with a volume of about 25 μl) or inverted (inverted pans with zero volume). The characteristics for each pan are listed in Table 1.

Values of R_{gap} and τ_{gap} were found from the shape of the melting endotherm of indium, which has a melting temperature of 156.60 °C and an

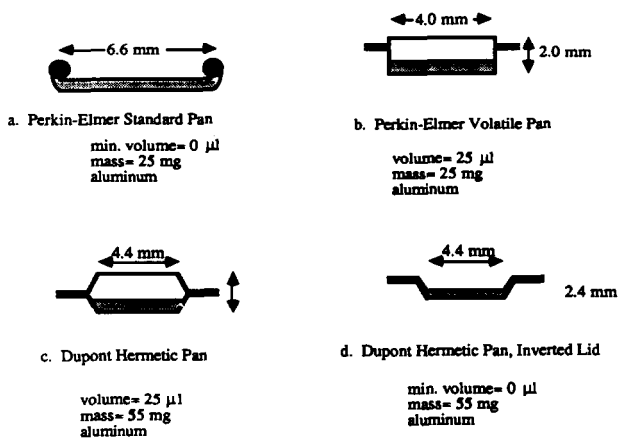

Fig. 4. DSC sample pans used in this work.

TABLE 1

Specifications of several DSC sample pans

Pan	Manufacturer	Material	m_p (mg)	vol (μl)	r_0 (mm)	m_pC_p (mJ K^{-1})	c
Standard	Perkin–Elmer	Al	25	$\geqslant 0$	3.3	24	4
Volatile	Perkin–Elmer	Al	25	25	2.0	24	1
Hermetic	Dupont	Al	55	25	2.2	53	1
Inverted	Dupont	Al	55	$\geqslant 0$	2.2	53	4

endothermic heat of fusion of 28.45 J g^{-1}. The DSC testing was done on a Perkin–Elmer DSC7, which operates by the power compensated principle. The R_{gap} and τ_{gap} values for each type of sample pan were determined by the shape of the indium melting peak, as shown in Fig. 5. Gray [26] found that the initial slope of the endotherm peak is $1/R_{gap}$, and after the peak the heat flow decays exponentially with time constant τ_{gap}:

$$\tau_{gap} = R_{gap}(m_pC_p + m_sC_s) \tag{8}$$

To measure τ_{DSC}, the onset temperature of the melting peak was measured at several scanning rates. The onset temperature T_m increased with S according to the relation

$$T_m(S) = T_m(0) + S(\tau_{DSC} + \tau_{gap}) \tag{9}$$

where $T_m(0)$ is the melting point at vanishingly small scanning rates. From eqn. (8), the slope of a plot of T_m vs. S is $\tau_{DSC} + \tau_{gap}$. Once τ_{gap} is determined from the melting endotherm, then τ_{DSC} can be found by subtraction.

RESULTS AND DISCUSSION

The discussion below will show (a) how the time lag of the DSC temperature controller and several types of sample pan may be evaluated, (b) calculation of the limiting heat flow for temperature control within 1° C,

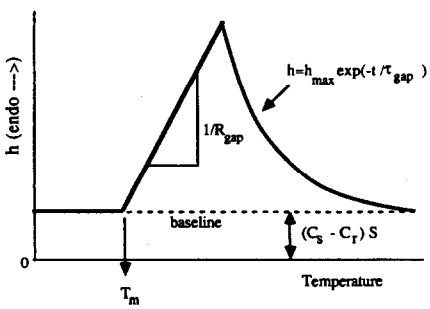

Fig. 5. DSC endotherm for determination of T_m, R_{gap} and τ_{gap}.

TABLE 2

Heat transfer characteristics of several DSC sample pans

Pan	R_{gap} (K mW^{-1})	τ_{gap} (s)
Standard	0.071	1.7
Volatile	0.083	2.0
Hermetic	0.060	3.2
Inverted	0.071	3.8

(c) the effect of time lag on heat flow measurement, and (d) an estimate of the mean temperature increase during peak exothermic heat flow. The DSC data used for illustration were for a vinyl ester resin (Dow Derakane 411-35LI) initiated by 113 mM *tert*-butyl peroctoate (Pennwalt). Testing was both isothermal (75 °C) and dynamic (10 K min^{-1}). The isothermal sample was large ($m_s = 25$ mg) to fill a volatile sample pan, hence displacing air from the headspace [27]. The mass of the dynamic DSC sample was 15 mg to prevent rupturing the seal in the volatile pan, as the sample expanded during heating.

Evaluation of pan and DSC time lags

Values of R_{gap} and τ_{gap} for the different sample pans are given in Table 2. The τ_{gap} is found from the exponential decay after the peak endotherm as shown in Fig. 5. According to Table 2, τ_{gap} is smaller for standard and volatile pans than for hermetic and inverted pans. These trends are consistent with eqn. (8), which predicts that τ_{gap} is proportional to the pan mass m_p and R_{gap}. Values of R_{gap} as determined from eqn. (8) show no trend with pan type (Table 2).

The melting temperature is plotted for several scanning speeds in Fig. 6 for standard and inverted pans. Subtracting τ_{gap}, given in Table 2, from the slopes of Fig. 6 the time lag τ_{DSC} is found to be 4.0 ± 0.1 s. It should be noted that both the inverted and the standard pans gave roughly the same value of τ_{DSC}, which confirms eqn. (9).

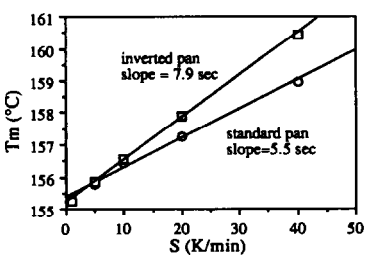

Fig. 6. Indium melting temperature as a function of scanning rate S and sample pan type.

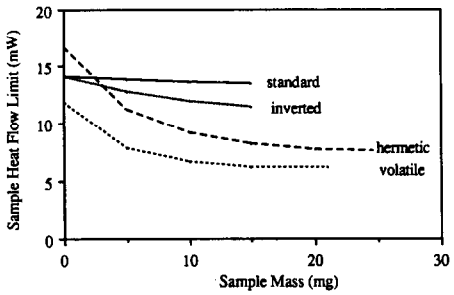

Fig. 7. Exothermic heat flow limit for control of average sample temperature to within 1°C under isothermal conditions.

Heat flow limits for mean temperature control within 1 °C

Temperature control is important for measuring the kinetics because reaction rates are temperature dependent. For example, the rate of initiation in a free radical polymerization typically has an activation energy of 125 kJ mol^{-1}, and hence a 1 K temperature increase at 70 °C results in a 14% increase in reaction rate. The maximum heat flow limit q_{max} for a ΔT_{limit} of 1 K as predicted from eqns. (5) and (7) are in Fig. 7. These calculations use a k_s of 4×10^{-4} cal cm^{-1} s^{-1} K^{-1} and ρ_s of 1.2 g cm^{-3}, which are values typical of the sample under study. Values of c and r_0 for each pan type are from Table 1. The lines of Fig. 7 stop at the mass required to fill each pan completely.

A greater ability to control sample temperature is manifested in Fig. 7 by a larger value of q_{max}. Hence, on the basis of Fig. 7 alone, the standard and inverted pans are the best pans for control of sample temperature. At zero sample mass (empty pans), the heat flow limit is proportional to $1/R_{gap}$, which from Table 2 is greatest for hermetic pans and least for volatile pans. However, these results change when the conduction resistance through the sample is considered. Because the lids of the standard and inverted pans contact the sample ($c = 4$), eqn. (5) shows that R_{sample} is smaller for these pans than for hermetic and volatile pans. Standard pans also have a large cross-sectional area; hence the samples are thinner for improved heat flow. Hence, q_{max} is greatest for standard and inverted pans when sample mass exceeds 5 mg. In hermetic and volatile pans, the sample does not contact the lid and the sample is insulated at the top surface. This restriction in heat flow results in q_{max} being lower than with standard and inverted pans.

Time lag correction for DSC data

With values of R_{gap} and τ_{DSC}, we may now use eqn. (2) to correct for time lag in DSC data. Typical isothermal DSC data for vinyl ester resin are

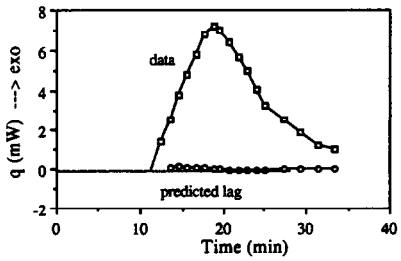

Fig. 8. Typical isothermal DSC data and predicted conduction lag correction.

given in Fig. 8. The conduction lag under these conditions is calculated from eqn. (2) and plotted in Fig. 8, approximating τ_{lag} to be 5 s. Clearly, the conduction time lag is much smaller than the heat flow from reaction, so conduction lag can be neglected under these conditions. The lag for dynamic DSC data (Fig. 9) is larger than in Fig. 8 because of the higher curing temperature and large values of dq/dt. By adding the correction to the data in Fig. 9, one can determine the expected exotherm if the time lag does not exist. However, as discussed next, large temperature errors in dynamic DSC experiments may also distort dynamic heat flow measurements.

Mean sample temperature

Figure 7 can be used to assess qualitatively the temperature increase due to exothermic heat flow during polymerization. For the isothermal DSC data in Fig. 8, the peak heat flow is about 7 mW. From Fig. 7, the sample heat flow limit for 25 mg samples in volatile pans is also about 7 mW, so the increase in mean sample temperature at the time of the peak exotherm is about 1° C. At times when sample heat flow is not at its peak, the mean temperature increase is smaller.

The data in Fig. 9 show a dynamic heat flow peak of 80 mW. From Fig. 7, the limiting heat flow for volatile pans with 15 mg samples is approximately 7 mW. Hence, the mean temperature increase at the peak exotherm in this run is approximately (80/7 =) 11° C, clearly a severe temperature increase.

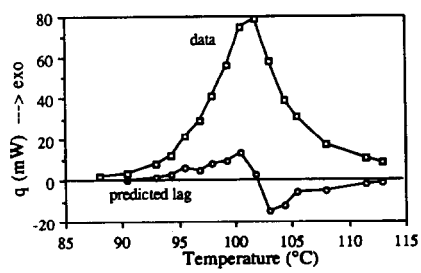

Fig. 9. Typical dynamic DSC data and predicted conduction lag correction.

Under these conditions, dynamic DSC data should not be used for kinetic characterization unless the peak heat flow is less than 7 mW. For highly exothermic reactions, very small samples may be necessary to decrease heat flow. Small samples, however, may create other errors due to evaporation, inaccurate sample mass, or, for free radical polymerization, oxygen in the pan headspace may prolong inhibition [27].

It should be noted that eqns. (4)–(7) assume that the temperature of the sample pan holder is at the programmed temperature. Some temperature deviation is always necessary, however, for the detection of heat flow. The increase in sample holder temperature during exothermic heat flow is additive to ΔT_{DSC} of eqn. (4), and hence increases in the mean temperature are underpredicted by the analysis. Closed-loop control, available on power compensated DSCs and some heat flux DSCs, will improve the ability of the DSC sample pan holder to maintain the desired temperature. Hence, these DSCs are preferred for kinetic studies over DSCs without closed-loop temperature control.

Selection of sample pan and sample mass

When selecting the sample pan for DSC, one should consider the ability of the DSC to control temperature and measure heat flow. An ideal DSC sample pan will have low mass, low heat capacity, a large cross-sectional area, a lid which is in contact with the sample, and seals to prevent sample loss. From Fig. 7, the standard pans have the best temperature control, but they are not well suited for volatile samples. Inverted pans pressurize the resin as it expands, and this pressurization may affect the reaction rate in unpredictable and irreproducible ways. Hence, the hermetic and volatile pans are best suited for volatile liquids because they prevent sample loss without excessive compression of the sample.

CONCLUSIONS

In this paper, the ability of the DSC to control temperature and measure heat flow was assessed. Heat flow measurement errors were due to both conduction resistance beneath the sample pan and the time lag of the DSC temperature control loop. Maintaining sample temperature during a large exotherm was hindered by heat flow resistance both beneath the sample pan and within the sample itself. A heat transfer model was used to predict the mean sample temperature during an exothermic reaction. DSCs with closed-loop control on sample temperature are generally preferred for kinetic characterization over DSCs without.

Standard sample pans had the best temperature control characteristics. With volatile samples, however, volatile or hermetic pans are necessary. The ideal sample pan will have low mass, a large cross-sectional area, a hermetic

seal, and a lid in thermal contact with the sample. For DSC studies of polymerization reactions, the heat flow limit for a 1°C mean sample temperature increase was estimated to be 7 mW for volatile and hermetic pans. Reaction kinetics measured for heat flows exceeding this limit may be in error. This limitation is especially severe for dynamic DSC runs, where sample heat flows are larger due to higher reaction temperatures. Small DSC sample sizes are recommended for highly exothermic samples.

ACKNOWLEDGMENTS

The authors would like to acknowledge the support for this work from the Dow Chemical Company (Freeport, TX), the Minnesota Productivity Center, and the Graduate School of the University of Minnesota.

APPENDIX: ANALYTICAL SOLUTION TO CONDUCTION IN A CYLINDER WITH GENERATION

Assuming that the time lag within a sample has a negligible effect on temperature, we can analyze heat flow under quasi steady state conditions, i.e. the sample temperature distribution is determined only by the instantaneous heat flow rate q. From Fourier's Second Law for heat conduction, the steady state temperature gradients are

$$\frac{\partial^2 T_r}{\partial z'^2} + \frac{1}{r'}\frac{\partial}{\partial r'}\left(r'\frac{\partial T_r}{\partial r'}\right) = -\frac{q\rho r_0^2}{k_s m_s} \tag{A.1}$$

where $T_r(r', z')$ is the difference between the sample temperature and the temperature of the pan, r_0 is the sample radius, m_s is the sample mass, and k_s is the sample thermal conductivity. Assuming that the sample is cylindrical, the sample thickness z is $m_s/\rho\pi r_0^2$. The dimensionless cylindrical coordinates are radius $r'(=r/r_0;\ 0<r'<1)$, and thickness $z'(=z/r_0;\ 0<z'<W$ where W is $z/r_0)$. The boundary conditions assume that the side and bottom walls are at the same temperature and that the top surface of the sample (which is not in contact with the lid) is insulating (Fig. 10):

$$T_r = 0 \text{ at } z' = 0 \tag{A.2}$$

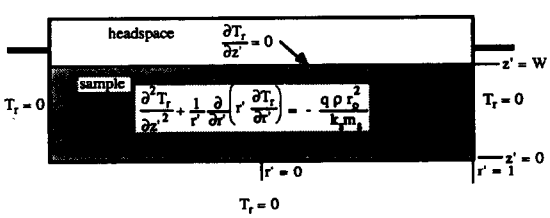

Fig. 10. Geometry for sample conduction model.

$$\partial T_r/\partial z' = 0 \text{ at } z' = w \tag{A.3}$$

$$T_r = 0 \text{ at } r' = 1 \tag{A.4}$$

$$T_r \text{ is finite at } r' = 0 \tag{A.5}$$

The homogeneous solution to eqn. (A.1) is the sum of terms with $\sin(\lambda_n z')$, where $\lambda_n = \pi(n - 1/2)/W$. Hence, the finite Fourier transform can be used to solve eqn. (A.1) [28]:

$$T_r(r', z') = \sum_{n=1}^{\infty} b_n(r') \sin(\lambda_n z') \tag{A.6}$$

where

$$b_n = \frac{2}{W}\int_0^w T_r(r', z') \sin(\lambda_n z')\, dz' \tag{A.7}$$

Equation (A.7) is used to transform eqn. (A.1) into an ordinary differential equation for b_n:

$$-\lambda_n^2 b_n + \frac{1}{r'}\frac{d}{dr'}\left(r'\frac{db_n}{dr'}\right) = -\frac{2r_0^2\rho q}{m_s k_s W \lambda_n} \tag{A.8}$$

and eqns. (A.4) and (A.5) become

$$\text{BC1: } b_n = 0 \text{ at } r' = 1 \tag{A.9}$$

$$\text{BC2: } b_n \text{ is finite at } r' = 0 \tag{A.10}$$

respectively. The homogeneous solution to eqn. (A.8) is a sum of homogeneous and particular solutions

$$b_n(r') = b_{n,h} + b_{n,p} = C_1 I_0(r'\lambda_n) - \frac{2r_0^2\rho q}{m_s k_s W \lambda_n^3} \tag{A.11}$$

where I_0 is the complex Bessel function [29] and C_1 is a constant. C_1 is found by using eqn. (A.9), and hence the solution for $b_n(r')$

$$b_n = \frac{2r_0^2\rho q}{m_s k_s W \lambda_n^3}\left[1 - \frac{I_0(r'\lambda_n)}{I_0(\lambda_n)}\right] \tag{A.12}$$

is inserted into eqn. (A.6) to find the temperature:

$$T_r(r', z') = \frac{2r_0^2\rho q}{m_s k_s W} \sum_{n=1}^{\infty}\left[1 - \frac{I_0(r'\lambda_n)}{I_0(\lambda_n)}\right]\frac{\sin(\lambda_n z')}{\lambda_n^3} \tag{A.13}$$

From eqn. (A.13) it is apparent that the maximum temperature is at the top center of the DSC sample, as expected:

$$T_{\max} = T_r(0, W) = \frac{2r_0^2\rho q W^2}{m_s k_s \pi^3} \sum_{n=1}^{\infty} \frac{(-1)^n}{(n - 1/2)^3} \tag{A.14}$$

The summation in eqn. (A.14) has an exact value of $\pi^3/4$; thus eqn. (A.14) can be simplified:

$$T_{max} = \frac{r_0^2 \rho q W^2}{2 m_s k_s} = \tfrac{1}{2} T_{char} \tag{A.15}$$

where

$$T_{char} = \frac{q \rho r_0^2 W^2}{k_s m_s} = \frac{qW}{\pi k_s r_0} = \frac{h_r}{\pi^2 k_s r_0^4 \rho} m_s^2 \tag{A.16}$$

and h_r is the heat of exotherm per unit mass. It should be noted from eqn. (A.16) that the mean temperature increases with the square of the sample mass. Therefore, as the DSC sample size doubles (say from 10 to 20 mg), the maximum temperature deviation T_{max} increases by a factor of 4. Thus, large DSC samples are prone to greater temperature errors if the sample is highly exothermic.

The expression for T_{char} in eqn. (A.16) is the worst case for DSC temperature control where the lid does not conduct heat. If the lid contacts the sample, and the temperature is uniform on the top and the bottom of the pan, then W, m_s and q are cut in half by symmetry, and T_{char} is reduced by a factor of 4. In general, T_{char} is given by

$$T_{char} = \frac{qW}{c \pi k_s r_0} \tag{A.17}$$

where $1 < c < 4$. Hence, when heat can conduct from the lid to the pan, T_{max} is roughly one-fourth the value when the lid is insulated.

The conduction resistance in the sample, R_{sample}, is defined as the bulk average sample temperature deviation $\langle T \rangle$ divided by heat flow q:

$$R_{sample} \equiv \langle T \rangle / q \tag{A.18}$$

where $\langle T \rangle$ is defined as

$$\langle T \rangle \equiv \frac{\int_0^W \int_0^1 T_r(r', z') r' \, dr' \, dz'}{\int_0^W \int_0^1 r' \, dr' \, dz'} = \frac{2}{W} \int_0^W \int_0^1 T_r(r', z') r' \, dr' \, dz' \tag{A.19}$$

Substituting eqn. (A.13) into eqn. (A.19), the integration over coordinates r' and z' can be performed separately:

$$\int_0^1 \left[1 - \frac{I_0(r' \lambda_n)}{I_0(\lambda_n)} \right] r' \, dr' = \tfrac{1}{2} - \frac{I_1(\lambda_n)}{I_0(\lambda_n) \lambda_n} \tag{A.20}$$

$$\int_0^W \sin(\lambda_n z') \, dz' = \frac{1}{\lambda_n} \tag{A.21}$$

TABLE 3

Values of $f(W)$ for eqns. (A.23) and (A.24)

W	$f(W)$	$Wf(W)$
0.05	7.61	0.38
0.06	7.50	0.45
0.07	7.40	0.52
0.08	7.30	0.58
0.09	7.20	0.65
0.1	7.09	0.71
0.2	6.21	1.24
0.3	5.36	1.61
0.4	4.59	1.84
0.5	3.92	1.96
0.6	3.34	2.00
0.7	2.85	2.00
0.8	2.45	1.96
0.9	2.11	1.89
1.0	1.83	1.83
2.0	0.61	1.22
3.0	0.29	0.87
4.0	0.17	0.68

Equations (A.13) and (A.19)–(A.21) are combined to give $\langle T \rangle$:

$$\langle T \rangle = \frac{4r_0^2 \rho q W^2}{m_s k_s \pi^4} f(W) = \frac{4}{\pi^4} T_{\text{char}} f(W) \tag{A.22}$$

where

$$f(W) = \sum_{n=1}^{\infty} \left[\frac{1}{2} - \frac{I_1(\lambda_n)}{\lambda_n I_0(\lambda_n)} \right] \frac{1}{(n - 1/2)^4} \tag{A.23}$$

Values of $f(W)$ are in Table 3. Hence R_{sample} is found by substituting eqns. (A.17) and (A.22) into eqn. (A.18):

$$R_{\text{sample}} \equiv \frac{\langle T \rangle}{q} = \frac{4}{\pi^5} f(W) \frac{W}{c k_s r_0} \tag{A.24}$$

This result is reported in eqn. (5).

REFERENCES

1 E.S. Watson, M.J. O'Neill, J. Justin and N. Brenner, Anal. Chem., 36 (1964) 1233.
2 R.C. Mackenzie and P.G. Laye, Chem. Br., 22 (1986) 1005.
3 R.B. Prime, in E. Turi (Ed.), Thermal Characterization of Polymeric Materials, Academic Press, New York, 1981.
4 R.A. Fava, Polymer, 9 (1968) 137.
5 H. Ng and I. Manas-Zloczower, Polym. Mater. Sci. Eng., ACS, 58 (1988) 1092.

6 T.A.M.M. Maas, Polym. Eng. Sci., 18 (1978) 29.
7 J.K. Gillham and C.C. Mentzer, J. Appl. Polym. Sci., 17 (1973) 1143.
8 K.E.J. Barrett, J. Appl. Polym. Sci., 11 (1967) 1617.
9 T.R. Cuadrado, J. Borrajo and R.J.J. Williams, J. Appl. Polym. Sci., 28 (1983) 485.
10 J.M. Salla and J.L. Martin, Thermochim. Acta, 126 (1988) 339.
11 S. Sourour and M.R. Kamal, Soc. Plast. Eng., Tech. Paper., 18 (1972) 93.
12 S. Sourour and M.R. Kamal, Thermochim. Acta, 14 (1976) 41.
13 P.W.K. Lam, Polym. Compos., 8 (1987) 427.
14 G.L. Batch and C.W. Macosko, Soc. Plast. Eng., Tech. Pap., 33 (1987) 974.
15 J.R. Ebdon and B.J. Hunt, Anal. Chem., 45 (1973) 804.
16 K. Horie, I. Mita and H. Kambe, J. Polym. Sci., Part A-1, 8 (1970) 2839.
17 S.Y. Pusatcioglu, A.L. Fricke and J.C. Hassler, J. Appl. Polym. Sci., 24 (1979) 937.
18 F. Cernec, U. Osredkar, A. Moze, I. Vizovisek and S. Lapanje, Makromol. Chem., 178 (1977) 2197.
19 W. Kostrzewski, Ph.D. Thesis, University of Pittsburgh, 1984.
20 G.W. Smith, Thermochim. Acta, 112 (1987) 289.
21 G. Widmann, Thermochim. Acta, 11 (1975) 331.
22 W.J. Sichina, Proc. NATAS Meeting, Washington, DC, September 27–30, 1987.
23 A.A. Duswalt, Thermochim. Acta, 8 (1974) 57.
24 U.F. Gonzalez and S.F. Shen, Soc. Plast. Eng., Tech. Pap., 33 (1987) 697.
25 M.J. O'Neill, Anal. Chem., 36 (1964) 1239.
26 A.P. Gray, in P.S. Porter and J.F. Johnson (Eds.), Analytical Calorimetry, Plenum, New York, 1968.
27 G.L. Batch and C.W. Macosko, Thermochim. Acta, 166 (1990) 185.
28 H.F. Weinberger, A First Course in Partial Differential Equations, Wiley, New York, 1965.
29 F.B. Hildebrand, Advanced Calculus for Applications, Prentice–Hall, Englewood Cliffs, NJ, 2nd edn., 1976.